proceedings

MDPI

Proceedings

Application of GNSS Methodologies to Obtain Precipitable Water Vapor (PWV) and Its Comparison with Radiosonde Data †

Raquel Perdiguer-López [1], José Luis Berné-Valero [2] and Natalia Garrido-Villén [2]

[1] Área de Ingeniería Cartográfica, Geodesia y Fotogrametría, Departamento de Explotación y Prospección de Minas, Universidad de Oviedo, 33007 Oviedo, Spain
[2] Área de Ingeniería Cartográfica, Geodesia y Fotogrametría, Universidad Politècnica de València, 46021 Valencia, Spain
* Correspondence: rperdiguer@uniovi.es
† Presented at the II Congress in Geomatics Engineering, Madrid, Spain, 26–27 June 2019.

Published: 25 July 2019

Abstract: A processing methodology with GNSS observations to obtain Zenith Tropospheric Delay using Bernese GNSS Software version 5.2 is revised in order to obtain Precipitable Water Vapor (PWV). The most traditional PWV observation method is the radiosonde and it is often used as a standard to validate those derived from GNSS. For this reason, a location in the north of Spain, in A Coruña, which has a GNSS station with available data and also a radiosonde station, was chosen. Two GPS weeks, in different weather conditions were calculated. The result of the comparison between the GNSS- retrieved PWV and Radiosonde-PWV is explained in the last section of this paper.

Keywords: GNSS meteorology; radiosounding; precipitable water vapor

1. Introduction

Global Navigation Satellite Systems have become a powerful tool in many scientific applications like Meteorology, where Precipitable Water Vapor (PWV) plays an important role and its variability is a key to understanding the hydrological cycle [1]. PWV can be measured by means of different methods using, e.g., radiosondes, Very Long Baseline Interferometry (VLBI) and GNSS. Bevis et al. [2] showed that PWV could be obtained from the tropospheric delay.

Using GNSS to obtain PWV have some advantages like high temporal resolution as well as high spatial resolution that is continually improving. Some studies have been carried out in Spain using GNSS to obtain PWV like Torres et al. [3] or Ortiz de Galisteo et al. [4].

The paper is structured as follows. Section 2 discuss the tropospheric delay and its relation to PWV. Section 3 describes the data and the processing strategy to obtain the variables. Finally, the results are given in Section 4.

2. Tropospheric Delay and Precipitable Water Vapor

The Troposphere is the lowest part of the atmosphere and the GNSS signal propagation in this neutral part depends on temperature, pressure and water vapor content. The tropospheric delay, once is transformed to the zenith direction, is called Zenith Total Delay (ZTD) and is usually divided into the sum of the dry part, called ZHD and the wet delay, ZWD, and can be estimated in the GNSS processing together with other parameters such as coordinates. ZHD can be accurately determined using the surface pressure of the site from empirical models and accounts for approximately 90 percent of the total delay while ZWD depends on the water vapor content and represents approximately the remaining 10 percent. Computing ZWD accurately is a difficult task because of the spatial and temporal variation of water vapor so, usually, ZWD is obtained from the subtraction of ZTD and ZHD. Relation between ZWD and PWV, using a conversion factor ∏, was demonstrated by Bevis [2]:

$$PW = \prod \times ZWD = \frac{10^6}{\rho R_V\left[\frac{k_3}{T_m}+k_2-mk_1\right]} \times ZWD \quad (1)$$

where ρ is the density of liquid water, R_v is the specific gas constant for water vapor, and m is the ratio of the molar masses of Water Vapor and dry air. The values of physical constants are $k_1 = (70.60 \pm 0.05)$ Kmb^{-1}, $k_2 = (70.40 \pm 2.2)$ Kmb^{-1} and $k_3 = (3.739 \pm 0.0012) \times 10^5$ K^2mb^{-1}. Also, factor ∏ depends on the water-vapor-weighted mean temperature, T_m. Determining T_m is very important to precise calculation of PWV because the relative error in the conversion factor ∏ will closely approximate the relative error in Tm [2]. This water-vapor-weighted mean temperature, T_m, can be determined using one of the following three methods:

1. With temperature and humidity profiles from either radiosonde observations or atmospheric reanalysis datasets, which is the most accurate option but its temporal resolution is quite low.
2. Using a relationship between surface temperature T_s and the water-vapor-weighted mean temperature T_m. This method requires of measurement of surface temperature and limited stations have surface temperature observed from ground meteorological sensors.
3. Calculating from an empirical model developed from atmospheric reanalysis products. Using these models allows to calculate the needed parameters without in situ meteorological data. In fact, the empirical model GPT2w requires only the position and height of the site, and the date as input parameters, providing the mean values plus annual and semiannual amplitudes of pressure as well as weighted mean temperature and other climatological parameters derived consistently from ERA-Interim field data with a horizontal resolution of 1° [5].

3. Data and Processing Strategy

3.1. GNSS Site

The present study is carried out with the data from the GNSS site ACOR in seaport of the city of A Coruña, in the north of Spain. This station (46°21′51″ N; 8°23′56″ W) belongs to Spanish network of the Instituto Geografico Nacional and contributes to the EUREF Permanent GNSS Network.

3.2. Radiosoundig Data

A radiosounding site (43.3658 N, 8.4214 W), belonging to AEMET, is located in A Coruña. To compare the information from the Radiosonde and the GNSS station the separation between them must be taking into account. Ohtani et al. [6] suggest the following conditions: (1) the horizontal distance between the two sites must be under 40 km and (2) the elevation difference within 100 m. GNSS station ACOR and Radiosonde Station, 08001, has a horizontal distance of 2 km approximately and 9 m in difference in elevation, so both requirements are come across.

The data from A Coruña radiosonde site was obtained from the Integrated Global Radiosonde Archive (IGRA) [7]. In particular, sounding-derived data archive was used.

3.3. Precipitable Water Vapor Processing

The first step in the PWV processing was the determination of ZTD. The calculation was based on a double-differencing (baseline) approach and was carried out by the Bernese GNSS software version 5.2 [8]. The main processing parameters are summarized in Table 1.

Table 1. Processing Parameters in Bernese GNSS Software.

Parameter	Bernese Processing
Frequency	GPS: L1, L2
Elevation Cutoff	3°
Sampling Rate	30 s
Satellite Orbit	Final IGS orbits
A priori troposphere model	GPT dry with GMF dry mapping
Mapping Function	Wet GMF
Tropospheric Gradients	Estimated
Gradient Model	CHENHER
Ambiguity Strategy	Quasi Ionosphere-Free (QIF)
Reference Frame	IGb08

Once GNSS Bernese processing was done and ZTD was calculated, next step was to obtain ZHD using the recommended [9] Saastamoinen Model with the pressure of the ACOR site obtained from GPT2w model. Then, ZWD was calculated from the subtraction of ZTD and ZHD. Finally, conversion factor $\prod$ was calculated to transform ZWD into PWV. The parameter T_m to calculate the conversion factor was also obtained from GPT2w model.

4. Results

The processing of GPS data allowed obtaining a value of the ZTD for each hour. Then, the temporal resolutions of PWV derived from GPS are 1 h while the radiosonde-retrieved PWV from IGRA dataset is sampled every 12 h. Accordingly, only PWV values at the common epochs are considered. Figure 1 shows the scatter diagrams of the GPS PWV and Radiosonde PWV while Table 2 lists the main results of the comparison of PWV from GNSS and Radiosonde data.

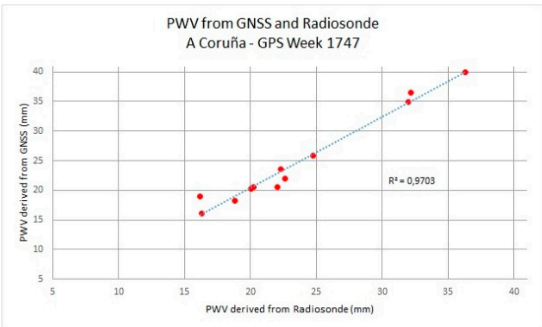

(**a**)

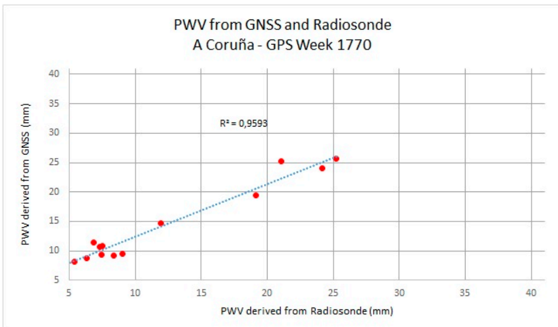

(**b**)

Figure 1. Comparison of PWV. (**a**) Scatter diagram of PWV derived from Radiosonde and GPS on 1747 GPS Week (**b**) Scatter diagram of PWV derived from Radiosonde and GPS on 1770 GPS Week. In both figures, the R2 correlation factor is included.

Table 2. Comparisons of the PWV estimated from GNSS and Radiosonde in A Coruña site.

Week	Maximum Difference (mm)	Minimum Difference (mm)	RMS (mm)	Correlation Coefficient r
1747	+4.40	−0.15	2.13	0.98
1770	+4.59	+0.09	2.64	0.98

The results shows that GPS-retrieved PWV and PWV derived from radiosonde agrees well, with a high correlation coefficient. The correlation coefficients obtained are consistent with the values found in Gui et al. [10] and Zhang et al. [11]. In general, GNSS-retrieved PWV are overestimated compared with PWV derived from Radiosonde. This result was also found in Gui et al. [10]. Table 2 shows that the differences between the two techniques are at the level of about few millimeters. The error on PWV derived from GNSS mainly come from the uncertainties in ZTD, in pressure (used to obtain ZHD) and in T_m (which is the main source of error in conversion factor Π). Many studies had been carried out to evaluate the uncertainties of retrieved PWV like Ning et al. [1]. Van Malderen et al. [12] established that the total uncertainty of GPS-retrieved PWV is less than 2 mm. As Table 2 shows, the RMS found in ACOR is 2.13 mm and 2.64 mm. The differences with those estimations could be due to the uncertainties of the PWV radiosonde data and the spatial and temporal separations between GNSS and radiosonde data. Similar results can be found in Ohtani et al. [9] (a little higher) or Zhang et al. [11] that found a mean RMS of 2.41 mm in a multiple comparison of PWV.

References

1. Ning, T.; Wang, J.; Elgered, G.; Dick, G.; Wickert, J.; Bradke, M.; Sommer, M.; Querel, R.; Smale, D. The uncertainty of the atmospheric integrated water vapor estimated from GNSS observations. *Atmos. Meas. Tech*. **2016**, *9*, 79–92, doi:10.5194/amt-9-79-2016.
2. Bevis, M.; Businger, S.; Chiswell, S.; Herring, T.A.; Anthes, R.A.; Rocken, C.; Ware, R.H. GPS Meteorology: Mapping Zenith Wet Delays onto Precipitable Water. *J. Appl. Meteor.* **1994**, *33*, 379–386, doi:10.1175/1520-0450(1994)033<0379:GMMZWD>2.0.CO;2 .
3. Torres, B.; Cachorro, V.E.; Toledano, C.; de Galisteo, J.P.O.; Berjón, A.; de Frutos, A.M.; Bennouna, Y.; Laulainen, N. Precipitable water vapor characterization in the Gulf of Cadiz region (southwestern Spain) based on Sun photometer, GPS, and radiosonde data. *J. Geophys. Res.* **2010**, *115*, D18103, doi:10.1029/2009JD012724.
4. Ortiz de Galisteo, J.P.; Bennouna, Y.; Toledano, C.; Cachorro, V.; Romero, P.; Andrés, M.I.; Torres, B. Analysis of the annual cycle of the precipitable water vapour over Spain from 10-year homogenized series of GPS data. *Q. J. R. Meteorol. Soc.* **2014**, *140*, 397–406, doi:10.1002/qj.2146.
5. Böhm, J.; Möller, G.; Shindelegger, M.; Pain, G.; Weber, R. Development of an improved empirical model for slant delays in the troposphere (GPT2w). *J. GPS Solut*. **2015**, doi:10.1007/s10291-014-0403-7.
6. Ohtani, R.; Naito, I. Comparisons of GPS-derived precipitable water vapors with radiosonde observations in Japan. *J. Geophys. Res.* **2000**, *105*, 26917–26929, doi:10.1029/2000JD900362.
7. National Center for Environmental Information. Available online: https://www.ncdc.noaa.gov/data-access/weather-balloon/integrated-global-radiosonde-archive (accessed on 1 May 2019).
8. Dach, R.; Lutz, S.; Walser, P.; Fridez, P. (Eds.) *Bernese GNSS Software Version 5.2. User Manual*; Astronomical Institute, University of Bern, Bern Open Publishing: Bern, Switzerland, 2015, ISBN: 978-3-906813-05-9, doi:10.7892/boris.72297.
9. IERS Conventions. *Frankfurt am Main: Verlag des Bundesamts für Kartographie und Geodäsie*; Petit, G., Luzum, B., Eds.; IERS Technical Note 36; 2010; p. 179, ISBN 3-89888-989-6.
10. Gui, K.; Che, H.; Chen, Q.; Zeng, Z.; Liu, H.; Wang, Y.; Zheng, Y.; Sun, T.; Liao, T.; Wang, H.; et al. Evaluation of radiosonde, MODIS-NIR-Clear, and AERONET precipitable water vapor using IGS ground-based GPS measurements over China. *Atmos. Res.* **2017**, *197*, 461–473.
11. Zhang, Q.; Ye, J.; Zhang, S.; Han, F. Precipitable Water Vapor Retrieval and Analysis by Multiple Data Sources: Ground-Based GNSS, Radio Occultation, Radiosonde, Microwave Satellite, and NWP Reanalysis Data. *J. Sens*. **2018**, *2018*, 3428303, doi:10.1155/2018/3428303.
12. Van Malderen, R.; Brenot, H.; Pottiaux, E.; Beirle, S.; Hermans, C.; De Mazière, M.; Wagner, T.; De Backer, H.; Bruyninx, C.: A multi-site intercomparison of integrated water vapour observations for climate change analysis. *Atmos. Meas. Tech.* **2014**, *7*, 2487–2512, doi:10.5194/amt-7-2487-2014.